Enhancement of Voltage Quality in Microgrid Using Fuzzy Controller

B. Dharma rao,
M.Tech (PS&A),
GITAM University,
Visakhapatnam, India,

A. Srinivasa Rao,
Professor, Department of EEE,
GITAM University,
Visakhapatnam, India

***Abstract* –The main purpose of this paper is to reduce the disturbances thereby improving voltage quality in the grid interfacing system by using Series/Shunt control strategy.**

The micro grid concept using renewable energy sources is a building block towards the future energy networks for long-term viable solutions of energy needs. The combination of wind energy and solar energy with local energy storage devices may reduce vulnerability to natural disasters because they do not require lifelines.

The energy from the Renewable energy sources (wind and solar) with local energy storage is connected to AC bus through Shunt and Series converters and this AC bus is connected to Utility Grid. Two three-phase four-leg inverters together with dc micro-sources and nonlinear loads are employed to construct a general series parallel grid-interfacing system.

The energy obtained from the renewable energy sources may contain harmonics and leads to distortion in output voltage. This distortions can be eliminated by using proper control strategies and filters in both the series and shunt converters.

Pulse Width Modulation (PWM) is used in both three phase four leg inverters. A conventional Proportional Integral (PI) and Fuzzy Logic Controllers are used for power quality enhancement by reducing the distortions in the output power.

The simulation results were compared among the two control strategies. With fuzzy logic controller and pi controller.

Keywords- Load Frequency Control, Two area interconnected power system, Conventional PI controller, Fuzzy Logic Controller.

1.INTRODUCTION

The integration of Renewable energy sources and energy storage systems has been one of the new trends in power electronic technology. The increasing number of Renewable energy sources and distributed generators require new strategies for their operations in order to maintain or improve the power supply quality and stability.

High prices of oil and global warming make the fossil fuels less and less attractive solutions. Wind power is a very important renewable energy source. It is free and not a polluter unlike the traditional fossil energy sources. It obtains clean energy from the kinetic energy of the wind, by means of the wind turbine .The wind turbine transforms the kinetic wind energy into mechanical energy through the drive train and then into electrical energy by means of the generator.

Fixed speed wind turbines are typically equipped with synchronous generators and connected to the load through power converters. The Fixed speed wind turbine directly drives the multi-pole permanent magnet synchronous generator (PMSG). It offers better performance due to its higher efficiency and less maintenance. PMSG can be used without a gearbox. When wind speed exceeds turbine rated speed, excess aerodynamic power should be limited in order to keep the shaft torque within its design limits. The electrical resulting power should also be controlled to maintain the dc voltage at a maximum value. There are two ways to control the excess power output from wind turbines. The primary braking system is mechanical and limits the aerodynamics forces (powers) on the turbine rotor above rated wind speed by changing the pitch angle of the blades. The secondary braking system is electrical, where the generator output is limited. Here maximum power point tracker system is used to extract the maximum power from the wind and it is connected to the load there by efficiency of the wind energy conversion system is increased.

Solar energy is also one of the important renewable energy source. Photo voltaic (PV) is a method of generating electrical power by converting solar radiation into direct current electricity using semiconductors that exhibit the photovoltaic effect. Photovoltaic power generation employs solar panels comprising a number of cells containing a photovoltaic material . There are different Tracking systems available for the solar panels. To get solar power more efficiently a Maximum Power Point Tracker (MPPT) is used that functions the photovoltaic (PV) modules in a way that allows the PV modules to produce all the power they are capable of. It is not a mechanical tracking system which moves physically the modules to make them point more directly at the sun. Since MPPT is a fully electronic system, it varies the module's operating point so that the modules will be able to deliver maximum available power. As the outputs of PV system are dependent on the temperature, irradiation, and the load characteristic

IJERT

MPPT cannot deliver the output voltage perfectly. For this reason MPPT is required to be implementing in the PV system to maximize the PV array output voltage.

This thesis focuses on the grid-interfacing architecture, taking into account how to interconnect Distributed Generation systems (DG systems) in the future grid with enhanced voltage quality. The desirable approach should be able to maintain high-quality power transfer between Distributed Generation system and the utility grid, and be able to improve the voltage quality at both user and grid side.[1]

2. GRID INTERFACING SYSTEM

Figure below shows an example of the future application of grid-interfacing converters. On the left-hand side, multiple Distributed Generation (DG) systems consisting of Solar Energy and Wind Energy together with energy storage and local loads are interconnected to construct a microgrid. The Energy storage systems (e.g., supercapacitor, battery, fuel cell, etc.) are used to store excess energy from the microgrid and send the stored energy back to the grid when needed, which are necessary for microgrid applications. [4]

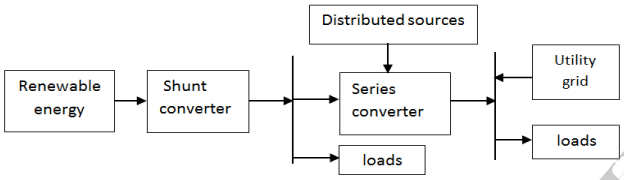

As a basic structure of the smart grid, plug-and-play integration of microgrids is essential, which can function whether they are connected to or separate from the electricity grid. On the right-hand side, a bidirectional series converter, which is supplied with distributed source and energy storage, interfaces the microgram to a utility grid (can be another micro grid) for exchanging power and isolates grid disturbances from each of the grids.

3. CONTROLLER DESIGN AND IMPLEMENTATION

Fig 3.1 and 3.2 shows the overall control structure of the series parallel system, which consists of reference signal generation and two individual controllers. A basic block, the symmetric sequence voltage detection and synchronization,is essential to determine the fundamental positive- and negative sequence voltage, as well as the grid frequency. This information is important for both converters in order to synchronize with the grid and to design control reference signals.[3]

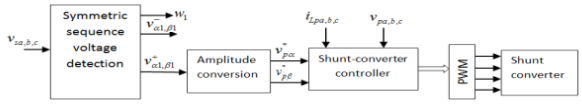

Fig 3.1Block diagram of overall control structure with Parallel converter

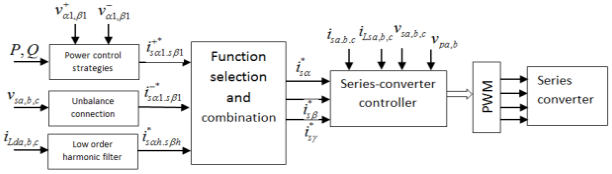

Fig 3.2 Block diagram of overall control structure with Series converter

As shown in Fig. 3.1 , based on the fundamental positive sequence grid voltages ($v^{+}_{\alpha 1}, v^{+}_{\beta 1}$) derived in the stationary frame, the amplitude conversion block first shapes the signals to per-unit quantities and then generates a set of reference signals ($v^{*}_{p\alpha}$, $v^{*}_{p\beta}$) with a specified amplitude for the parallel converter.
The series converter is applicable for achieving multi-level control objectives. Hence, the block "function selection and combination" in Fig. 3.2 indicates that different objectives can be integrated into the system by choosing appropriate reference signals $i^{*}_{s\alpha}, i^{*}_{s\beta}, i^{*}_{s\gamma}$. Details about the unbalance correction scheme, which is used to generate current reference for negative-sequence voltage compensation. For the power control strategy, which are used to obtain desired currents for active/reactive power transfer. Due to the space limitation, they are not duplicated here. The active filter function is represented by the block "loworder harmonics filter". References of low-order current harmonics, denoted by $i^{*}_{s\alpha h.s\beta h,s\gamma h}$, can be obtained. In order to track the desired reference signals, the rest of this section presents the main design aspects of the series and parallel converter control.

3.1 Control of the parallel converter:

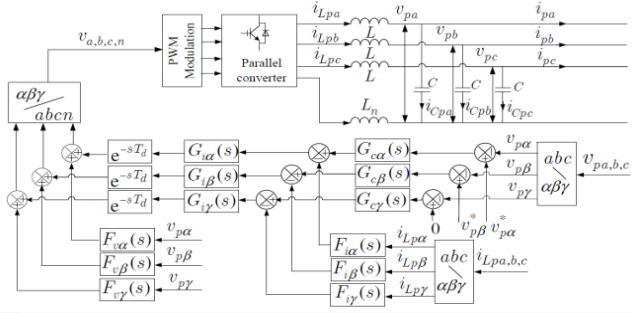

Fig 3.3 Control diagram of the parallel converter

IJERT

The control diagram of the parallel-converter is shown in Fig. 3.3, where the sampling and transfer delay of the control is considered and represented by e^{-sTd} . System parameters are provided in the section of experimental results. Simplifying the inverter to have a unity gain, the average model of the α-quantities in the proposed control scheme is shown in Fig.3.4 In the stationary frame, the α, β, and γ quantities are decoupled and their control designs are similar.[1]

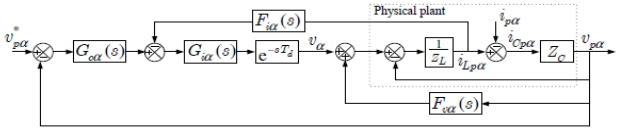

Fig.3.4 Block diagram representation of the α-quantities in Fig.3.3

3.1.1System Instability Improvement:

A voltage feed forward loop can usually be used to improve system dynamics. It is shown in this section that this loop can also eliminate the instability of parallel converters under no-load conditions. When the parallel converter is not connected to local loads and also does not deliver power to the grid, the output current *ipα* in Fig. 3.4 equals to zero. The transfer function of the physical plant (from the inverter output *vα* to the filter output *vpα*) in Fig.3.4 can be expressed as

$$G_{p\alpha}(s) = \frac{v_{p\alpha}}{v_{\alpha}} = \frac{Z_C}{Z_L + Z_C}$$

with *ZL* = *sL* + *RL* and *ZC* = *RC* + 1 *sC* , where *RL* and *RC* are the equivalent series resistors (ESR) of *L* and *C*, Respectively
Taking in to account the sampling and transfer delay in the feed forward loop , it follows that

$$F_{v\alpha}(s) = K_{ff} e^{-sT_d} \approx K_{ff} \frac{1 - sT_d/2}{1 + sT_d/2}$$

Where is the forward gain , is the sampling period ,In order to observe the effect of the feed forward loop on the physical plant , the inductor current loop is excluded by setting , therefore after including the voltage feed forward loop , the transfer function from to is obtained as

$$G_{pl-ff}(s) = \frac{v_{p\alpha}}{v_{\alpha}} = \frac{G_{pl}}{1 - G_{pl}F_{v\alpha}(s)}$$

Frequency response of $G_{pl-ff}(s)$ are plotted with different κ_{ff} , if κ_{ff} =0 , then $G_{pl-ff}(s) = G_{pl}(s)$, a sharp increase of the amplitude and a 180degree phase shift appear at the resonance frequency of the LC filter tank. This limits the control band width and also makes the controller design difficult.

Selective harmonic regulation: Before studying the inner current-loop, the external voltage control-loop is first analyzed. Because the adopted grid-interfacing system is a four-wire system and will be explored with asymmetrical nonlinear loads, triplen odd harmonic components will also appear in the line. In order to prevent the output voltage from being distorted under nonlinear load conditions, multiple PR controllers are employed as compensators for voltage regulation at selected harmonic frequencies, expressed as by

$$G_{c\alpha}(s) = K_p + \sum_{n=1,3,5}^{9} \frac{2w_{bn}K_{In}s}{S^2 + 2w_{bn}s(nw_c)^2}$$

where the resonant terms at 1st, 3rd, 5th, 7th, and 9th harmonics are selected, with KP = 0.55,KI1 = 50,KI3,5,7,9 = 20, ωb1 = 10 rad/s, ωb3,5,7,9 = 6 rad/s, and ωc = 314 rad/s. It can be seen that the open-loop gains at selected frequencies are enhanced so as to fully compensate the voltage harmonics at these frequencies.

3.1.2Disturbance Sensitivity Improvement*:*

The inner current loop is used to improve system sensitivity to the disturbances on the output current ipα. Since the voltage regulation loop plus the feedforward loop have already pushed the system bandwidth to 1.2 kHz with a phase margin of 20◦, the inner current compensator Giα(s) can hardly increase the bandwidth. In order to maintain the characteristics of the system control at low-order harmonic frequencies, a unity gain is assigned to the inner current regulator, that is Giα(s) = 1, and only high-frequency components of the inductor current are sampled. Thus, current feedback loop is expressed as[1]

$$G_{i\alpha}(s) = K_{fI} \frac{s}{s + 2\pi f_{hp}}$$

where *KfI* is the current feedback coefficient and *fhp* the high pass bandwidth. the system sensitivity to current disturbances can be obtained, i.e.

$$G_d(s) = \left. \frac{v_{p\alpha}(s)}{i_{p\alpha}} \right|_{v^*_{p\alpha}=0}$$

IJERT

3.2 Control of the series converter:

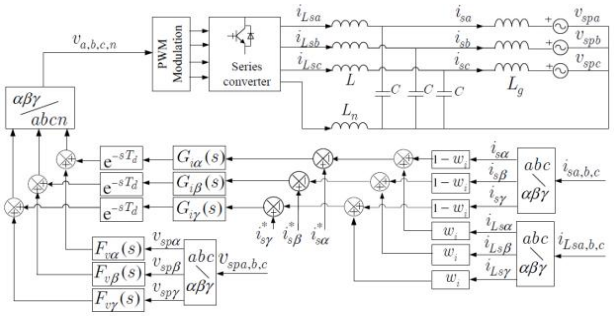

Fig 3.5 Control diagram of the Series converter

The control consists of a voltage feed forward loop and a current feedback-control loop. As an additional voltage feed forward loop, it is used to decouple the influence of grid voltage disturbances on the output current isα, thereby improving system dynamics. Fvα(s) is simply a unity gain. In the rest of this subsection, only the current feedback-control loop is specified.

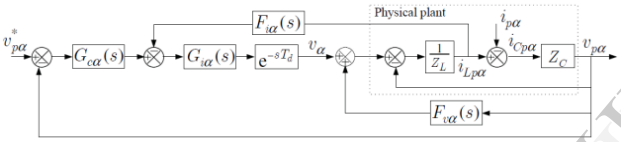

Fig 3.6 Block diagram representation of the small-signal model

Disregarding the ESRs of the inductor and the grid impedance, the transfer function from the inverter output voltage to the inductor current and the grid current are expressed, respectively, as

$$G_{v2i_L}(s) = w_i \frac{L_g cs^2 + 1}{LL_g cs^3 + (L + L_g)s}$$

and

$$G_{v2is}(s) = \frac{i_{s\alpha}}{V_\alpha} = \frac{1}{LL_g cs^3 + (L + L_g)s}$$

By introducing a weighting factor *wi* for the two currents, from the above figure, the modified system transfer function from the inverter output voltage *vα* to feedback current *ifα* is obtained, i.e.

$$G_{v2i_f}(s) = w_i \frac{L_g cs^2 + 1}{LL_g cs^3 + (L + L_g)s} + (1 - w_i) \frac{1}{LL_g cs^3 + (L + L_g)s}$$

When wi = 0, the control model in Fig. 3.6 represents grid current feedback control, and when wi = 1, it represents inductor current feedback control

$$G_{v2i_f}(s) = \frac{1}{sL_{sum}}$$

Therefore, the third-order system is turned into a first-order system, implying that the resonance problem is eliminated. For the purpose of suppressing harmonic currents, the current compensator *Giα*(*s*) is designed with the multiple PR controller . In the experiment, the resonant terms are only selected at the 1st, 3rd, 5th, and 7th harmonic frequencies.

3.3 FUZZY LOGIC CONTROLLER

Fuzzy controllers are normally built with the use of fuzzy rules. Fuzzy rules are conditional statement that specifies the relationship among fuzzy variables. These rules help us to describe the control action in quantitative terms and have been obtained by examining the output response to corresponding inputs to the fuzzy controller. The basic block diagram of Fuzzy Logic Controller is shown below.

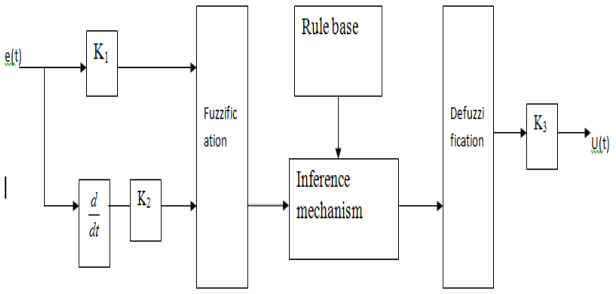

Fig.3.7 Block diagram of Fuzzy Logic Controller

The Fuzzy Logic Controller is applied in Load Frequency control of Two area system, this analysis is done using different Fuzzy based rules using Linguistic variable i.e., by considering Three variable and Five variable[4]

IJERT

Error rate /Error	LP	MP	SP	VS	SN	MN	LN
LP	PB	PB	PB	PM	PM	PS	Z
MP	PB	PB	PM	PM	PS	Z	NS
SP	PB	PM	PM	PS	Z	NS	NM
VS	PM	PM	PS	Z	NS	NM	NM
SN	PM	PS	Z	NS	NM	NM	NB
MN	PS	Z	NS	NM	NM	NB	NB
LN	Z	NS	NM	NM	NB	NB	NB

Table 3.1 Seven variable rule base

L(e,ce) = {NB,NM,Z,PM,PB,NS,PS}

Where NB = Negative Big

NM = Negative Medium

Z = Zero

PM = Positive Medium

PB = Positive Big

PS= Positive Small

NS= Negative Small

The type membership functions here used are Triangular type and the membership function range is -1 to 1 i.e., universe of discourse. The defuzzification is done by using Centroid method. The seven variable rule base consisting of 49 rules and are If –Then type.

4. SIMULATION AND RESULTS

The parameters of the system are given in Table 5.1

Description	Symbol	Value
Rated grid voltage	$V_{ga,b,c}$	230V/50Hz
Grid impedance	Z_g	2 mH (ESR 0.628 Ω)
Output inductor	L	1.8 mH (ESR 0.03 Ω)
Output capacitor	C	5 μF
Neutral inductor	L_n	0.67 mH (ESR 0.02 Ω)
Series transformer	T_N	1 : 1
dc-link voltage	V_{dc}	750 V
dc-link capacitors	C_{dc}	4400 μF
Switching frequency	f_{sw}	16 kHz
Sampling frequency	f_{sp}	8 kHz

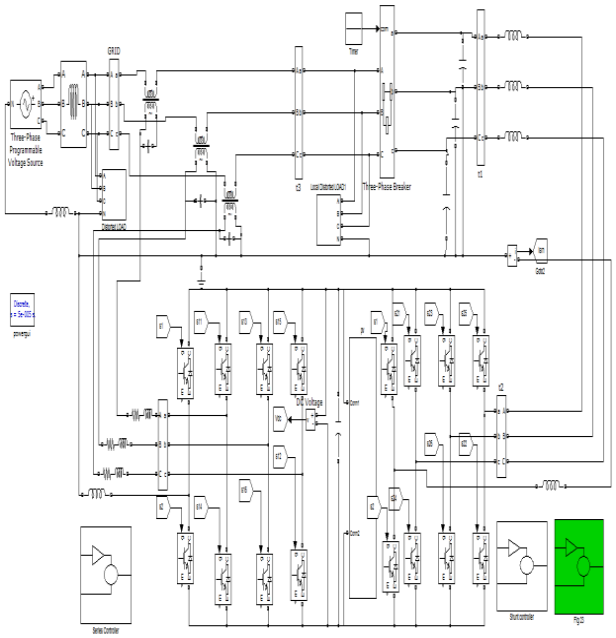

Fig 4.1Simulation implementation of Micro Grid

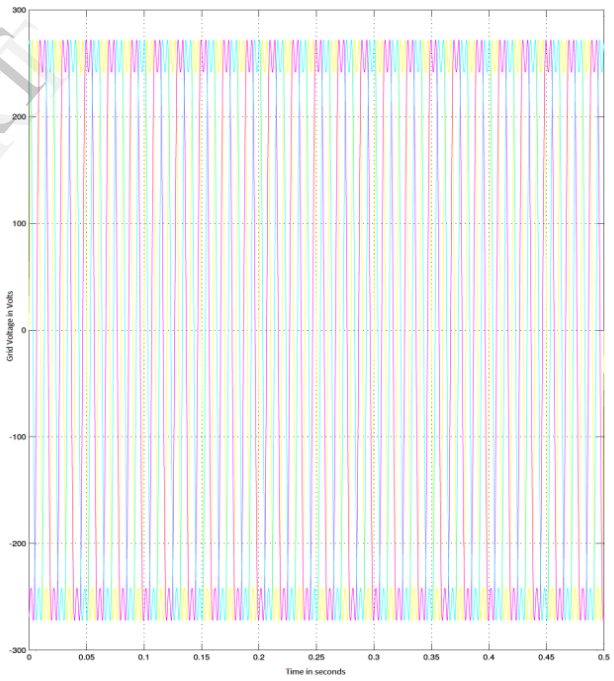

Fig 4.2 Grid voltages of the series- parallel system under a distorted grid is 8% from 0 to 0.5 with 3rd and 5th harmonic's

IJERT

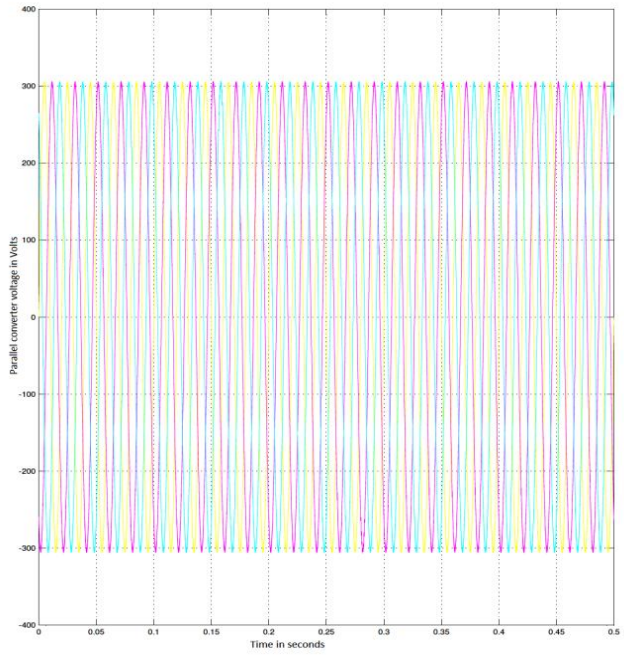

Fig 4.3output voltage of the parallel converter of the series- parallel system under a distorted grid with 2% from 0 to 0.5 sec.with 310v

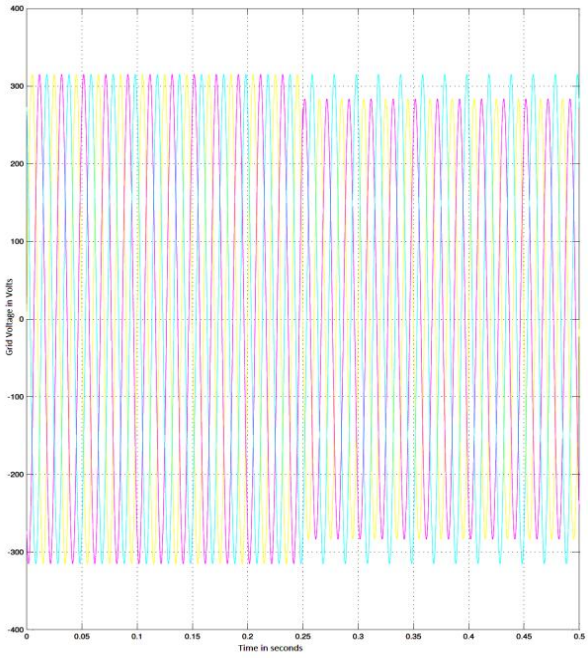

Fig 4.5 grid voltage of the series-parallel system under unbalanced Voltage dips accrued in Phase A and B at 0.25sec to0.5sec with 7% distrotion

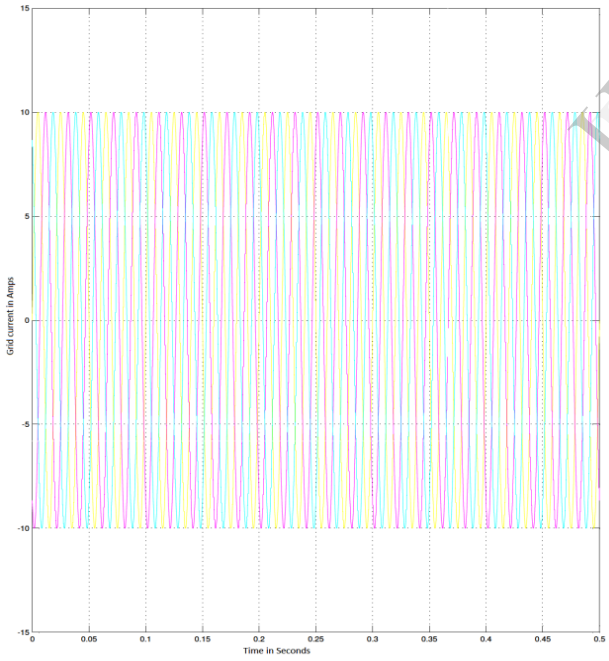

Fig 4.4 grid current of the series- parallel system under a distorted grid current is 2% with 10A current

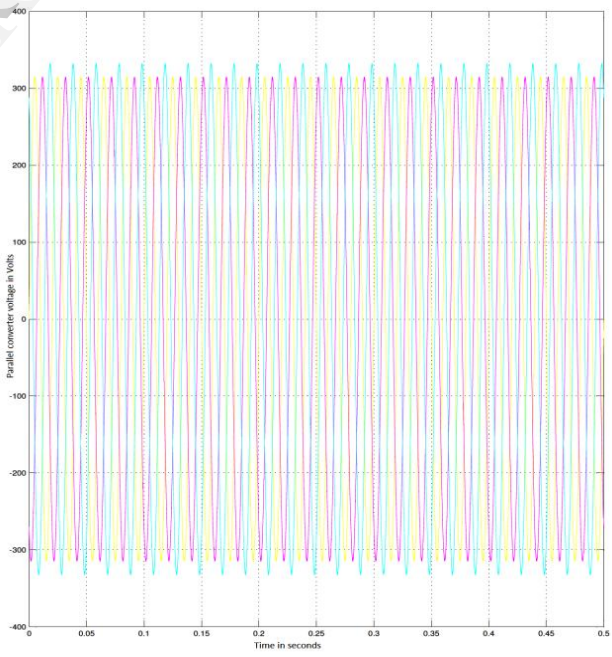

Fig 4.6 output voltage of the parallel converter of series-parallel system under unbalanced voltage dips accrued from 0 to 0.5sec from Pahse A and B with 10%.

IJERT

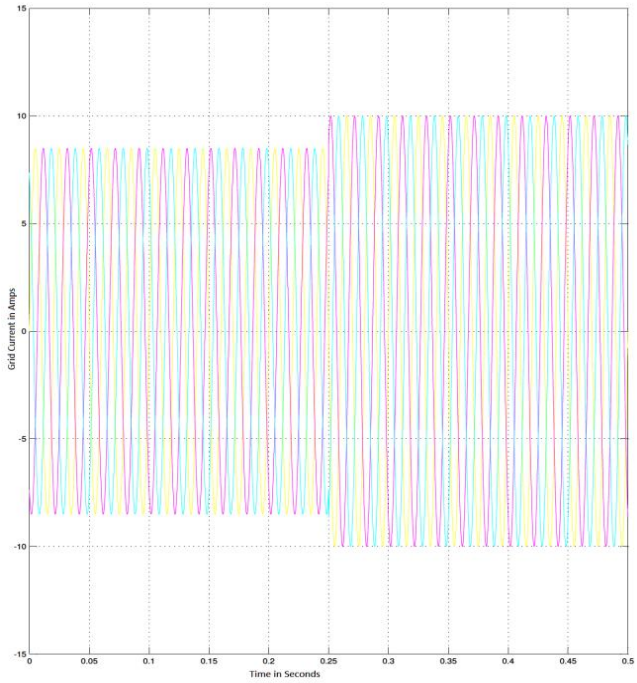

Fig 4.7 Grid current of the series-parallel system under unbalanced voltage dips from 0 to 0.25sec with 10% magnitude of 10Amps

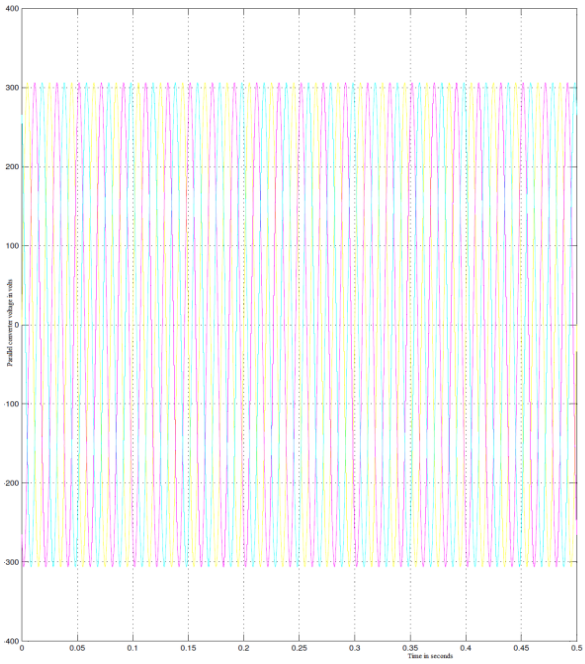

Fig 4.9 output voltage of the parallel converter of series-parallel system under unbalanced voltage dips compensated with fuzzy controller using with 2% distortion

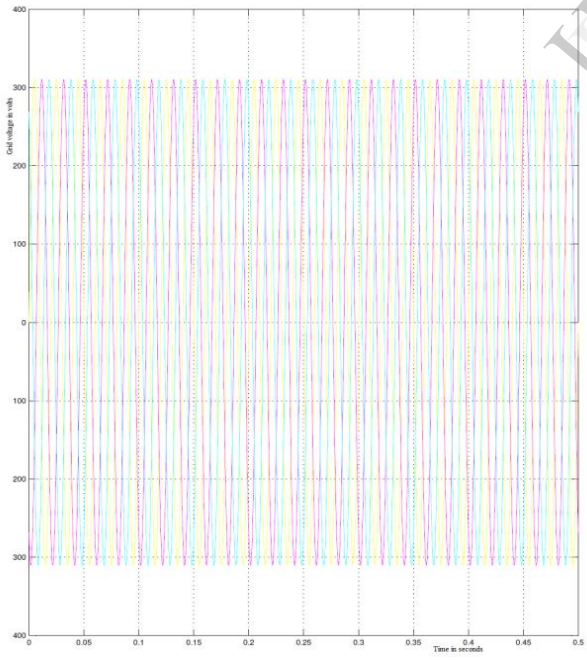

Fig 4.8 grid voltage of the series-parallel system under unbalanced voltage dips compensated with fuzzy controller with 2%distrotion

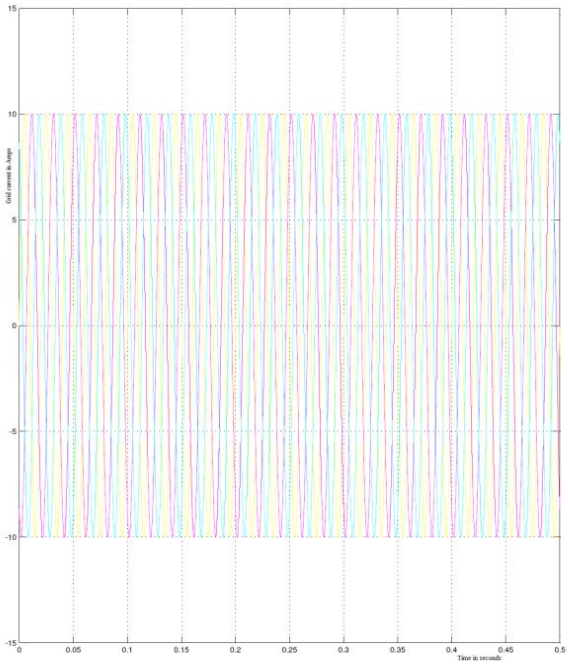

Fig 4.10 Grid current of the series-parallel system under unbalanced voltage dips compensated with fuzzy controller using Pq theory technique with 2% distortion.

IJERT

VI. CONCLUSION

The simulation results obtained for the Grid interfacing using series and parallel converter system with conventional PI controller and Fuzzy logic controller.

Due to the presence of non-linearity's in the system, harmonics will produce which leads to voltage distortions. Hence from "Fig 4.2 Grid voltages of the series- parallel system under a distorted grid", 8% distortions during time interval 0.25 sec to 0.5sec with 3^{rd} and 5^{th} harmonics were observed.

By using conventional PI controller in the system we can reduce these distortions. Fig 4.5 to 4.7 shows the simulation results obtained with PI control technique.

" In Fig 4.5 grid voltage of the series-parallel system under unbalanced Voltage dips ", Voltage dips occurred in phase A and Phase C during time interval of 0.25sec to 0.5sec with 7% distortions .

"In Fig 4.6 output voltage of the parallel converter of series-parallel system under unbalanced voltage dips", Voltage dips occurred in phase A and Phase C during 0 to 0.5sec with 10 % distortions .

"In Fig 4.7 Grid current of the series-parallel system under unbalanced voltage dips",we can observe that 10% distortions during time interval of 0-0.25sec.

Since the conventional PI controller has been designed with fixed gains, it failed to provide the best control performance . This drawback can be overcome by adopting fuzzy set theory.

Fig 4.8 to Fig 4.10 are the simulation results with fuzzy logic controller. Hence From the simulation results obtained with Fuzzy control strategy we can observe that the voltage distortions are reduced to 2% which is negligible.

To improve the Voltage quality further we can go for most advanced controllers like Artificial Neural Network (ANN) controller, Adaptive Neuro Fuzzy Inference System(ANFIS) controller etc.,

VII. REFERENCES

[1] F.Wang, J. L. Duarte, and M. A.M. Hendrix, "Grid-Interfacing Converter Systems with Enhanced Voltage Quality for Microgrid Application Concept and Implementation" IEEE 2011.

[2] F.Wang, J. L. Duarte, and M. A.M. Hendrix, "Control of grid-interfacing inverters with integrated voltage unbalance correction," in Proc. IEEE Power Electronics Specialists Conference, 2008, pp. 310-316.

[3] F. Wang, J.L. Duarte, and M.A.M. Hendrix, "Pliant active and reactive power control for grid-interactive converters under unbalanced voltage dips," IEEE Transactions on Power Electronics, in press, 2010.

[4] H. Farhangi, "The path of the smart grid," IEEE Power Energy Mag.,vol. 8, no. 1, pp. 18-28, Jan./Feb. 2010

[5] H. Fujita, and H. Akagi, "The unified power quality conditioner: the integration of series- and shunt-active filters," IEEE Trans. Power Electron., vol. 13, no. 2, pp. 315-322, Mar. 1998

[6] S. Silva, P.F. Donoso-Garcia, P.C. Cortizo, and P.F. Seixas, "A three phase line-interactive ups system implementation with series-parallel active power-line conditioning capabilities," IEEE Trans. Ind. Appl., vol. 38, no. 6, pp. 1581-1590, Nov./Dec. 2002.

[7] B. Han, B. Bae, H. Kim, and S. Baek, "Combined operation of unified power-quality conditioner with distributed generation," IEEE Trans. Power Delivery, vol. 21, no. 1, pp. 330-338, Jan. 2006.

[8] H. Tao, "Integration of sustainable energy sources through power electronic converters in small distributed electricity generation systems," PhD dissertation, Eindhoven university of technology, 2008.

[9] D. Graovac, V. A. Katic, and A. Rufer, "Power quality problems compensation with universal power quality conditioning system," IEEE Trans. Power Delivery, vol. 22, no. 2, pp.968-976, Apr. 2007.

[10] Y.W. Li, D.M. Vilathgamuwa, and P.C. Loh, "Microgrid power quality enhancement using a three-phase four-wire grid-interfacing compensator," IEEE Trans. Ind. Appl., vol. 41, no. 6, pp. 1707-1719, Jul. 2005.

[11] J.M. Guerrero, L.G.D. Vicuna, J. Matas, M. Castilla, and J. Miret, "A wireless controller to enhance dynamic performance of parallel inverters in distributed generation systems," IEEE Trans. Power Electron., vol. 19, no. 5, pp. 1205-1213, Sept. 2004.

[12] Y.W. Li, D. M. Vilathgamuwa, and P.C. Loh, "Design, analysis, and real-time testing of a controller for multi bus micro grid system," IEEE Trans. Power Electron., vol. 19, no. 5, pp. 1195-1204, Sept. 2004.

[13] Y.W. Li, and C.-N. Kao, "An accurate power control strategies for power-electronic-interfaced distributed generation units operating in a low-voltage multi bus micro grid," IEEE Trans. Power Electron., vol. 24, no. 12, pp. 2977-2988, Dec. 2009.

IJERT